Optimization of pulsed electrodeposition of aluminum from $AlCl_3$-1-ethyl-3-methylimidazolium chloride ionic liquid

Jinwei Tang*, Kazuhisa Azumi

Graduate School of Engineering, Hokkaido University, N13W8, Kitaku, Sapporo 060-8628, Japan

*Corresponding Author: Tel: +81 11706 6749; Fax: +81 11706 7897.

E-mail address: tangjw1984@gmail.com.

Birth date: 1984.05.15.

Abstract

In this study, Al was electrodeposited on a platinum substrate at room temperature from an ionic liquid bath of EMIC containing $AlCl_3$ using potentiostatic polarization (PP), galvanostatic polarization (GP), monopolar current pulse polarization (MCP) and bipolar current pulse polarization (BCP). Transition of current or potential during galvanostatic or pulse polarization revealed that the initial stage of the deposition process was controlled by a nucleation process depending on the polarization condition. For example, the average size of Al deposits decreased with increasing current density in the case of GP. FE-SEM observation showed that dense and compact Al deposits with a smooth surface were obtained by the current pulse method. Roughness factor evaluated from electrochemical impedance measurement confirmed the smooth surface of these deposits. Adhesion strength of Al deposits was greatly improved by using BCP in which an anodic pulse was combined with a cathodic pulse for electrodeposition. In this study, the optimal parameters for BCP were found to be I_C = -16.0 mA cm^{-2}, I_A = 1.0 mA cm^{-2}, r_C (duty ratio) = 0.5, and f = 2 Hz. The mechanisms of electrodeposition by these three methods are discussed.

***Key words**:* Ionic liquid, Aluminum, pulsed electrodeposition

1. Introduction

Aluminum and its alloys have low density and high levels of corrosion resistance and electric conductivity and are thus promising materials for various applications. Because of the high corrosion resistivity of Al, various methods for Al coating of corrodible materials have been developed. Compared with physical deposition methods such as thermal spray coating [1], physical or chemical vapor deposition [2], electroless plating [3] and hot dipping [4], the electrodeposition method has many advantages such as low energy consumption, low cost, simple operation, and better control of the microstructure of deposited layers. However, Al coatings cannot be electrodeposited in an aqueous solution because water decomposes prior to Al deposition. Room temperature ionic liquids (RTIL) have many unique features such as low vapor pressure, good ionic conductivity and a wide electrochemical potential window, and they have recently been considered as media for Al electrodeposition [5-6]. One of the ionic liquids used for electrodeposition of Al is a mixture of 1-ethyl-3-methyl-imidazolium chloride (EMIC) and aluminum chloride ($AlCl_3$), from which various metals and alloys, such as Al, Al-Zn [7], Al-Mo-Ti [8], and even AlInSb semiconductor [9], have been electrodeposited. In this acidic ionic liquid, it has been suggested that the dominant ions of $Al_2Cl_7^-$ are electrochemically reduced to form metallic deposits according to the following reaction [6]:

- (1)

The pulse current technique has been used for electrodeposition of aluminum [10-12] because it enables the properties and structures of deposits to be controlled and improved by adjusting pulse parameters such as frequency, duty ratio, pulse intensity and polarity. Yang [10] studied the effects of the electrolyte composition, current density and current form on characteristics of Al layers deposited from a molten salt system of $AlCl_3$-n-butylpyridinium chloride and found that more compact and smoother layer was obtained with pulse current method compared with DC method. Li et al. [11] also investigate the effects of pulse parameters on Al electrodeposits from $AlCl_3$-EMIC ionic liquid containing $NdCl_3$, and found that the micro-deposits changed from polygonal to spherical crystals as increasing DC and the pulse current gave the brighter and flatter deposits compared with the DC method with the same average current density.

Despite the potential improvement of aluminum deposition using the pulse technique and ionic liquids, there has been no fundamental and systematical investigation of the pulse polarization process and optimization of pulse conditions. In the present work, therefore, prior to explore the electrodeposition condition of Al on the other metals such as Mg and steels for corrosion protection, an Al layer was electrodeposited on a Pt substrate from EMIC/$AlCl_3$ ionic liquid using various polarization conditions including potential and current pulse technique, and the results were compared to clarify the deposition process and to obtain optimum deposition conditions.

2. Experimental

The ionic liquid [EMIm]Cl (Aldrich, BASF quality, purity ≥ 95%) was dried at 373 K in vacuum for 24 h and stored in a glove box filled with nitrogen gas. Anhydrous $AlCl_3$ powders (JUNSEI Chemical Co., purity ≥98.0%) were used as a source of Al without further purification. An electrodeposition bath composed of $AlCl_3$ and [EMIm]Cl with a molar ratio of 2:1 was prepared by slow addition of $AlCl_3$ to [EMIm]Cl in a beaker at room temperature with stirring. Some fumes and heat were generated during preparation, and then a slightly dark-brown liquid was obtained. For further purification, an Al foil (≥ 99.999%) was immersed in the bath for 3 days to remove residual water by water decomposition reaction accompanied by hydrogen gas evolution [13]. Finally, a transparent liquid with a slightly yellow color as an electrodeposition bath was obtained.

In the electrodeposition process, a typical three-electrode system composed of a working electrode (WE) of Pt foil (7×7 mm), a reference electrode (RE) of Pt wire or Al wire (99.99%), and a counter electrode (CE) of an Al plate (99.999%) was used. In this paper, electrode potential is presented as a value vs. Al-RE. Before experiments, the WE was cleaned in water by ultrasonic cleaning for 5 min followed by acetone rinsing and then dried with a stream of air. Then the WE was immediately transferred into the glove box and immersed in the ionic liquid bath for 20 min prior to polarization. The WE was then polarized between 1.0V and 2.0V (vs. Pt-RE) with a scan rate of 0.1 Vs^{-1} to remove adsorbed impurities [6].

A potentio/galvanostat (Ivium Technologies, model IviumStat) was used for electrochemical operations such as electrodeposition, cyclic voltammetry and electrochemical impedance spectroscopy (EIS). Electrodeposition of Al was conducted using galvanostatic polarization (GP), monopolar current pulse (MCP), or bipolar current pulse (BCP) polarization. A voltammogram was measured with potential scanning from open circuit potential (OCP, approximately 1.1 V vs. Al-RE) toward the negative direction. EIS measurement of Al deposits was conducted by applying an ac signal of 0.05 V_{P-P} (Considerable noise appeared below this amplitude.) in the frequency range of 1-10^5 Hz in borate buffer solution (0.15M H_3BO_3 and 0.05M $Na_2B_4O_7$, pH 8.5) [14] to evaluate surface roughness of deposits. All experiments were conducted at room temperature. Microstructures of surfaces and cross sections of deposits were observed using a field emission scanning electron microscope (FE-SEM, JEOL Co., model JSM-6500).

3. Results and discussion

3.1 Voltammetry

Typical voltammograms of a Pt substrate at various scan rates in [EMIm]Cl/$AlCl_3$ are shown in **Fig.1**. Al deposition in the cathodic scan and its stripping in the anodic scan can be clearly seen in the figure. Al deposition potential was lower than -0.2 V, indicating that relatively large nucleation overpotential was necessary. Both the deposition and stripping current of Al were enhanced by increasing the scan rate. Appearance of a current peak during the cathodic scan at a relatively slow scan rate indicates the formation of a depletion layer of Al ions around the Pt-WE. In the anodic scan, a shoulder peak around 0 V became more apparent as the scan rate decreasing, which may be attributed to the formation of depression layer of $AlCl_4^-$ on WE necessary for Al dissolution. The following clear peak and abruption of anodic current were completion of Al deposits dissolution.

Dependence of cathodic and anodic current peaks on square root of the scan rate is shown in **Fig.2**. The linear relationship for the cathodic current peak indicates that the deposition rate was determined by the diffusion process. Deviation of peaks from the linear line at high scan rates was attributed to insufficient growth of the diffusion layer due to a fast potential sweep.

Fig. 3 shows the coulombic efficiency of Al deposition, i.e., ratio of anodic charge consumed by Al dissolution against the cathodic charge during the cathodic polarization, as a

function of square root of the scan rate. The efficiency increased and then decreased with increase in scan rate. Relatively low efficiency at a low scan rate indicates that the contribution of a side reaction other than the deposition reaction becomes apparent. This side reaction is thought to be related to impurities in the organic solvent such as residual water or oxygen dissolved from incompletely deaerated atmosphere in the glove box [15]. Decrease in efficiency at a higher scan rate was caused by growth of a depletion layer of Al ions on the electrode surface, which also accelerates the side reaction due to insufficient supply of Al ions.

3.2 Potentiostatic polarization (PP)

Chronoamperometry at the initial stage of electrodeposition provides useful information on nucleation and growth processes. Typical current-time transients of Pt-WE during cathodic PP are shown in **Fig. 4** as a function of polarization potential. The large cathodic current in the first part of the transition was due to sudden deposition of Al to form nuclei, and the following decrease was caused by formation of a depletion layer of Al ions. The subsequent increase of deposition current was caused by nuclei growth, which enabled efficient collection of Al ions due to a steric effect. The behavior of the deposition current in the following stage depended on the deposition potential. At a potential higher than -0.4 V, a diffusion layer of Al ions formed near the Pt-WE and the thickness of the layer was balanced with the constant deposition rate. On the other hand, at a potential lower than -0.5 V, the continuously decreasing deposition current indicates continuous growth of the diffusion layer due to a higher rate of Al ion consumption. The required time to reach the transition from the nucleation stage to the diffusion control stage, τ, is indicated in the figure. The value of τ decreased with lowering of the deposition potential, indicating rapid completion of the nucleation stage at a higher deposition rate.

3.3 Galvanostatic polarization (GP)

Variation of electrode potential during GP at various current densities is shown in **Fig. 5**. Polarization potential became less-noble with increasing deposition current. The initial potential showed a drop for a few seconds as shown in a time-expansion plot. This characteristic behavior of potential transition corresponds to the nucleation process shown in Fig. 4, and the duration of this nucleation stage became short with increasing deposition current.

SEM micrographs of the Al surface electrodeposited using GP at various current densities are shown in **Fig. 6**. Higher magnification images are also shown as insets. At current density of -3.0 mA cm^{-2} shown in **Fig. 6a**, Al deposits were composed of flake-like particles with poor adherence and roughly covered the substrate surface. At -4.5 mA cm^{-2} shown in **Fig. 6b,** the deposits became fine but were still porous. Compact and dense deposits continuously covering the substrate were obtained at -6.0 mA cm^{-2} as shown in **Fig. 6c**. Deposits obtained at -8.0 mA cm^{-2} showed smooth and dense surface composed of finer particles as can be seen in **Fig. 6d**. It is evident that the average size of deposit particles decreased with increasing current density. This tendency can be explained by the model in which initial deposition of Al at low current density occurs only on limited sites due to low overpotential and each deposit grows slowly due to the low deposition rate. On the other hand, at high current density, initial deposition of Al occurs at various sites due to large deposition overpotential, and further deposition occurs at other sites to form new deposits rather than growth of pre-deposits because of the high deposition rate. In the cross-sectional SEM image of sample d shown in **Fig. 6e**, dense and compact deposits of approximately 9 μm in thickness were obtained, although some of the deposits had already detached from the Pt substrate due to poor adhesion.

3.4 Monopolar current pulse polarization (MCP)

An example of the current pulse waveform and corresponding potential response during MCP is shown in **Fig. 7**. During the resting period, t_{Off}, potential remained around E_1. When a cathodic current was applied during t_C, the potential shifted suddenly to a less-noble value, E_2, and then moved gradually in the less-noble direction reaching E_3 at the end of t_C. Increase of the electrodeposition overpotential during t_C corresponds to growth of a depletion layer on the surface at each cycle. Introduction of t_{Off} after t_C provided recovery of surface concentration of Al ions as confirmed from the fact that E_2 restituted at each cycle. Characteristic parameters of potential transient are summarized in **Table 1**. From this table, it is clear that a small duty ratio (r_C), i.e., the portion of polarization time in one whole cycle, $r_C = t_C/(t_C + t_{Off})$, provides a small potential difference, $\Delta E_1 = E_1 - E_2$ and $\Delta E_2 = E_2 - E_3$, i.e., suppression of Al ion depletion and thus efficient Al deposition to obtain better deposits.

SEM images of the Al surface electrodeposited on Pt from the [EMIm]Cl/$AlCl_3$ bath using MCP with different values of r_C and frequency, f, are shown in **Fig. 8**. The cathodic current

for Al deposition was kept constant at -16 mA cm^{-2} while r_C and f were changed. In all cases, a dense and compact microstructure is clearly observed compared with the case of GP shown in Fig. 6. Surface morphology of MCP deposits changed with changes in r_C and f. For example, the surface became smooth with increase in t_{Off} at fixed t_C and with decrease in t_C at fixed t_{Off}. Improvement of Al deposits with decrease in r_C can be explained by the recovery of Al ion concentration on the surface during t_{Off} and thus the suppression of side reactions, resulting in a better deposition condition in the next t_C duration. The smoothest deposit was obtained in the case of **Fig. 8c** in which smallest r_C was applied. The cross-sectional SEM image of the specimen in **Fig. 8f** shows a compact and dense structure of Al deposits with a thickness of about 8 μm.

3.5 Bipolar current pulse polarization (BCP)

An example of the current pulse waveform and corresponding potential response in the BCP polarization is shown in **Fig. 9**. In this procedure, improvement in uniform deposition is induced by partial dissolution of deposits during the slightly anodic polarization pulse for t_A after interruption of cathodic deposition pulse for t_C. The potential transient was similar to that for MCP shown in Fig. 7. The potential E_1 was more noble than that for MCP and moved gradually in a noble direction during t_A. The less-noble value of E_1 with about -0.2V than that of Al-RE during anodic dissolution of Al deposits indicated that Al deposits were more active than the Al plate used as an RE. When polarization was switched from anodic to cathodic, the potential difference, $\Delta E_2 = E_2 - E_3$, was much smaller than that of MCP and remained almost constant during t_C. This indicates that the overpotential of Al deposition reaction was lessened in the case of the BCP method, probably due to alteration of the Al surface after slight anodic dissolution and good supply of Al ions to the surface provided by additional Al dissolution during t_A to the supply of Al ions via diffusion layer. As a result, the depletion effect of Al ions on the surface during t_C was weakened and thus better electrodeposition conditions such as lower overpotential for electrodeposition and small contribution of side reactions were obtained.

Morphology of the Al surface electrodeposited using the BCP method with the conditions of I_C = -16 mA cm^{-2}, $r_C = t_C/(t_C + t_A) = 0.5$, f = 2 Hz and various values of anodic current density, I_A, during anodic polarization time, t_A, is shown in **Fig. 10**. The deposit surface became smooth with increasing I_A. This was probably can be confirmed from the value of roughness factor, γ,

shown in **Table 1** obtained by EIS measurement as described below. The value of γ is similar to the value measured for deposits obtained by the MCP method shown in Table 1. However, adhesion strength of the BCP films was considerably improved compared with that of the MCP films. For example, the MCP film was easily detached from the substrate in the tape test, while the BCP film was not. The reason for the better adhesion strength of BPC films is that partial dissolution of the deposit surface during the anodic pulse period makes a fresher surface for the following deposition under the condition of presence of impurities in the ionic liquid bath such as a small amount of oxygen or water. **Fig.10d** shows a cross-sectional image of aluminum on the Pt substrate. The uniform and dense Al layer adhered properly on the substrate and exhibited excellent deposition quality. As shown in this figure, the thickness of the deposited layer was approximately 9 μm, which is very close to the theoretical value calculated from Faraday's electrolysis law. This result suggested that the thickness of the deposit could be easily controlled by adjusting the total charge passed. Therefore, it is proposed that the BCP method is better for obtaining Al deposits with a smooth surface and better adhesivity.

3.6 Comparison of the three electrodeposition methods

In this subsection, Al deposits formed by the GP, MCP and BCP methods are compared. As seen in SEM images of Al deposits, surface morphology depends on electrodeposition condition. EIS was thus applied to quantitatively evaluate the surface roughness of Al deposits. The Al surface is always covered with an air-formed oxide film in the atmosphere. Assuming that the thicknesses of the oxide films formed on the Al deposits and Al plate are identical, the roughness factor of Al deposits can be evaluated from the capacitance value. In this evaluation, impedance spectra of WE were fitted by the calculation curve using an equivalent circuit, and the capacitance value of the deposits was compared with the value measured for the Al plate [16]. EIS results of all samples show similar appearance as can be seen in **Fig. 9**. The equivalent circuit used for simulation of impedance response was composed of an electrolyte resistance, R_S, a charge transfer resistance, R_F, and a constant phase element, *CPE*, which is a capacitor with compensation of non-uniformity of the electrode surface. The impedance of a *CPE*, Z_{CPE}, is given by

n ,

where j is an imaginary unit, ω is an angular frequency of the applied ac signal, and A and n are variables. Since the value of n was 0.92-0.96, being close to 1, a *CPE* can be considered to be a capacitor. The capacitance of the air-formed oxide film on the deposited Al, C_F, is given by the following equation:

$$d\ ,$$

where ε is the permittivity of vacuum, ε_f is permittivity of an oxide layer, γ is the roughness factor of the deposited film and A is the geometric surface area. The value of γ was assumed to be 1 for the flat Al foil. The total capacitance, C_T, can be expressed as follows:

$$H\ ,$$

where C_H is capacitance of the Helmholtz layer. In the present study, C_H (a typical value of C_H for most metals is in the range $C_H \approx$ 10–100 μF cm^{-2}) can be neglected for rough estimation of γ because it is considerably larger than C_F (a typical value of C_F is ca. 3.6 μF cm^{-2}). The value of γ was determined from the ratio of the capacitance of deposits to that on the flat Al foil as shown in **Table 1**. Decrease of γ with decreasing r_C confirms that a smoother surface was obtained at smaller r_C, as can be seen in the SEM images shown in Fig. 8.

Electrodeposition processes in the three polarization methods are schematically presented in **Fig. 12**. In the GP method, Al particles grow continuously after the initial nucleation process, which occurs only on limited sites due to low overpotential at low current density as shown in Fig. 6. Although the density of Al deposits is improved at relatively high current density, adhesivity of Al deposits remains poor. In the MCP method, a large current density during t_C enables initial nucleation of Al deposits with high density on the surface. In the following stage, recovery of Al ion concentration during t_{Off} weakens the growth of the depletion layer. This provides further Al deposition on various sites of the surface in the successive plating cycle, t_C, resulting in dense and smooth deposits. In the BCP method, however, not only density and smoothness but also adhesion strength of Al deposits are improved. These improvements are probably due to the following factors: (1) good supply of Al ions to the surface, which enables uniform deposition, (2) refreshing of the Al deposit surfaces during slight anodic dissolution, which removes active sites for preferential Al deposition and thus uniformizes deposition conditions of the surface to enable deposition reaction on many sites, resulting in lower overpotential for deposition reaction, and (3) suppression of side reactions due to lowering of overpotential such as adsorption of organic compounds, which may disturb crystal growth and/or

formation of bonding between deposits and pre-deposits. These possibility need to be clarified by further investigation in the future.

4. Conclusions

In this study, electrodeposition of Al from Lewis acidic 1-ethyl-3-methyl-imidazolium chloride EMIC/$AlCl_3$ (0.5 mol%) ionic liquid onto a Pt substrate at room temperature was investigated by using potentiostatic polarization (PP), galvanostatic polarization (GP), monopolar current pulse polarization (MCP) and bipolar current pulse polarization (BCP). The following conclusions could be drawn from the experimental results:

1) The deposition process was controlled by the initial nucleation stage and following deposit-growth stage. The former was affected by the polarization method and current density, and the latter was also affected by the current density via formation of a diffusion layer of Al ions.

2) Surface morphology and particle size of Al deposits can be controlled by the polarization conditions. For example, particle size becomes small with increase in current density in the GP method. Duty ratio and frequency are also adjusted to obtain dense deposits composed of small Al particles in the current pulse polarization method. Generally, the current pulse polarization method provides dense deposits with a smooth surface.

3) The initial nucleation process and following growth process of Al deposits can be optimized by adjusting the wave form of the current pulse. For example, adhesion strength of Al deposits was improved by adding slight anodic dissolution in the current pulse cycle. The best Al deposits with a smooth surface and good adhesion were obtained in the conditions of I_C = -16.0 mA cm^{-2}, I_A = 1.0 mA cm^{-2}, r_C = 0.5, and f = 2 Hz in the BCP method.

Acknowledgment

This work was supported by the Global COE Program (Project No. B01: Catalysis as the Basis for Innovation in Materials Science) from the Ministry of Education, Culture, Sports, Science and Technology, Japan, and also supported in part by the Light Metal Educational Foundation.

References

[1] O. Sarikaya, S. Anik, S. Aslanlar, S.C. Okumus, E. Celik, *Mater. Des*., **28** (2007) 2443.

[2] J.H. Yun, B.Y. Kim, S.W. Rhee, *Thin Solid Films*, **312** (1998) 259.

[3] N. Koura, H. Nagase, A. Sato, S. Kumakura, K. Takeuchi, K. Ui, T. Tsuda, and C. K. Loong, *J. Electrochem. Soc.*, 1**55** (2008) D155.

[4] W.J. Cheng, C.J. Wang, *Surf. Coat. Technol*., **204** (2009) 824.

[5] J.K. Chang, S.Y. Chen, W.T. Tsai, M.J. Deng, IW. Sun, *Electrochem. Conmmun.*, **9** (2007) 1602.

[6] T. Jiang, M.J. Chollier Brym, G. Dubé, A. Lasia, G.M. Brisard, *Surf. Coat. Technol.*, **201** (2006) 1.

[7] S.J. Pan, W.T. Tsaia, J.K. Chang, IW. Sun, *Electrochim. Acta*, **55** (2010) 2158.

[8] T. Tsuda, S. Arimoto, S. Kuwabata, C.L. Hussey, *J. Electrochem. Soc.*, **155** (2008) D256.

[9] T. Tsuda, C.L. Hussey, *Thin Solid Films*, **516** (2008) 6220.

[10] C.C. Yang, *Mater. Chem. Phys.*, **37** (1994) 355.

[11] B. Li, Y. Chen, L.G. Yan, J.D. Ma, *Electrochemistry*, **78** (2010) 523.

[12] G. Manoli, Y. Chryssoulakis and J.C. Poignet, *Plating and Surf. Finish.*, **78** (1991) 64.

[13] J. Vaughan, D. Dreisinger, *J. Electrochem. Soc.*, **155** (2008) D68.

[14] H.H. Elsentriecy, K. Azumi, H. Konno, *Electrochim. Acta*, **53** (2008) 4267.

[15] P.K. Lai, M. Skyllas-Kazacos, *J. Electroanal. Chem.*, **248** (1988) 431.

[16] M.T. Tanvir, Y. Aoki, H. Habazaki, *Thin Solid Films*, **517** (2009) 6711.

Table 1. Parameters of current pulse polarization as duty ratio (r_C), frequency (f), cathodic current density (I_C), anodic current density (I_A), potential response (E_1, E_2, ΔE_1, ΔE_2), capacitance (C_F) and roughness factor (γ) of Al deposit films.

Sample	r_C	f /Hz	I_C /mA cm^{-2}	I_A /mA cm^{-2}	E_1 /V	E_2 /V	ΔE_1 /V	ΔE_2 /V	C_F /mF m^{-2}	γ
MCP-a	0.5	3.3	16	0	-0.27	-0.64	0.37	0.08	22.37	2.28
MCP-b	0.375	2.5	16	0	-0.25	-0.60	0.35	0.05	21.04	2.14
MCP-c	0.23	1.54	16	0	-0.24	-0.56	0.32	0.04	17.86	1.82
MCP-d	0.33	1.33	16	0	-0.24	-0.61	0.37	0.09	19.13	1.95
MCP-e	0.5	1	16	0	-0.26	-0.59	0.33	0.10	20.72	2.11
BCP-a	0.5	2	16	0.3	-0.24	-0.58	0.34	0.02	22.90	2.33
BCP-b	0.5	2	16	0.5	-0.23	-0.56	0.33	0.02	20.80	2.12
BCP-c	0.5	2	16	1.0	-0.21	-0.53	0.32	0.01	15.69	1.59
Al foil	–	–	–	–	–	–	–	–	9.81	1

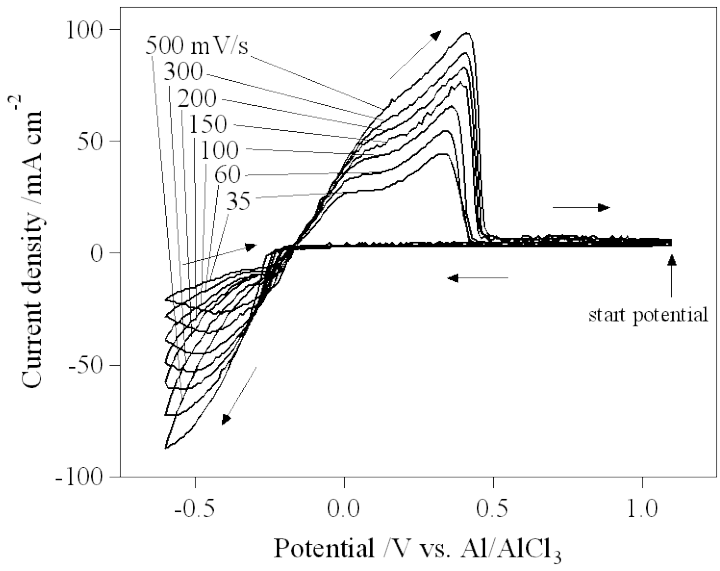

Fig. 1 Cyclic voltammograms of Pt in the [EMIm]Cl/$AlCl_3$ (0.5 mol%) plating bath measured with scan rates of 35, 60, 100, 150, 200, 300, and 500 mV s^{-1}.

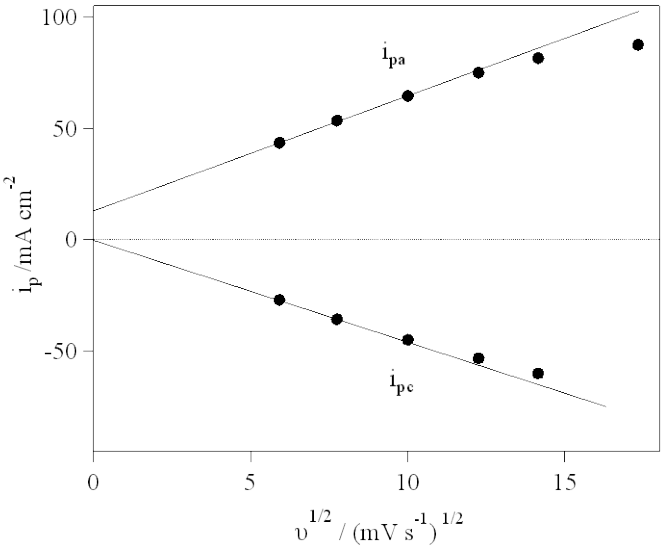

Fig. 2 Relationship between cathodic peak current (i_{pc}) and anodic peak current (i_{pa}) against square root of the scan rate (υ) obtained from the data shown in Fig. 1.

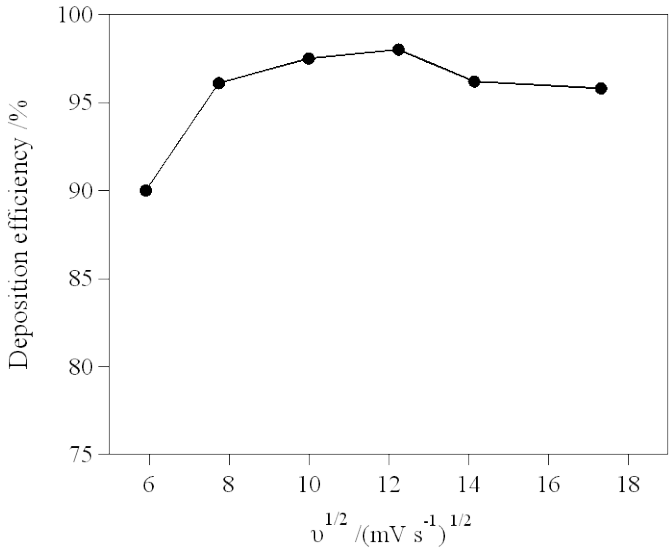

Fig. 3 Efficiency of Al electrodeposition against square root of the scan rate (υ) during the potential scan shown in Fig. 1.

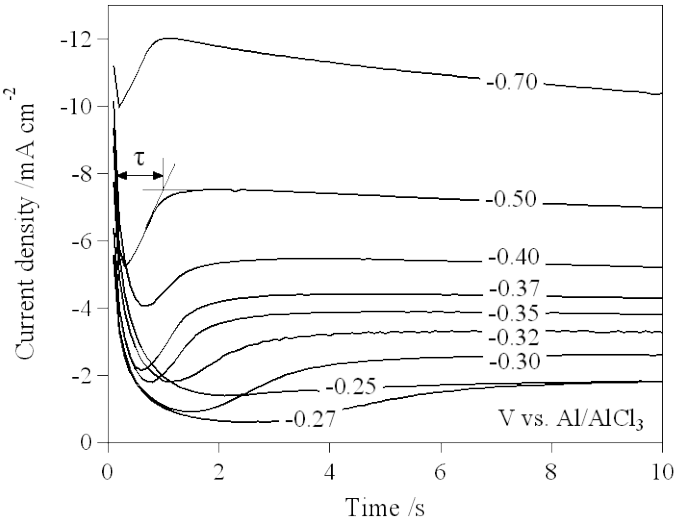

Fig. 4 Current-time transient of Pt-WE during potentiostatic cathodic polarization in the [EMIm]Cl/$AlCl_3$ (0.5 mol%) bath at various potentials.

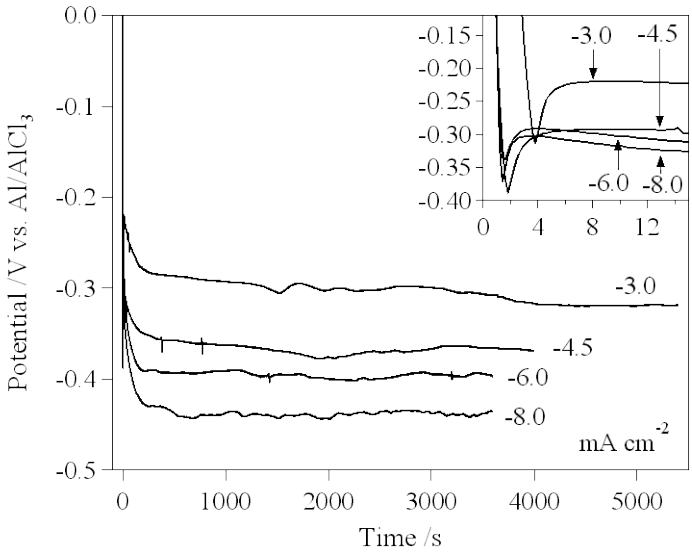

Fig. 5 Potential-time transition of Pt electrode during galvanostatic polarization for Al electrodeposition in the EMIm]Cl/$AlCl_3$ (0.5 mol%) bath at various current densities.

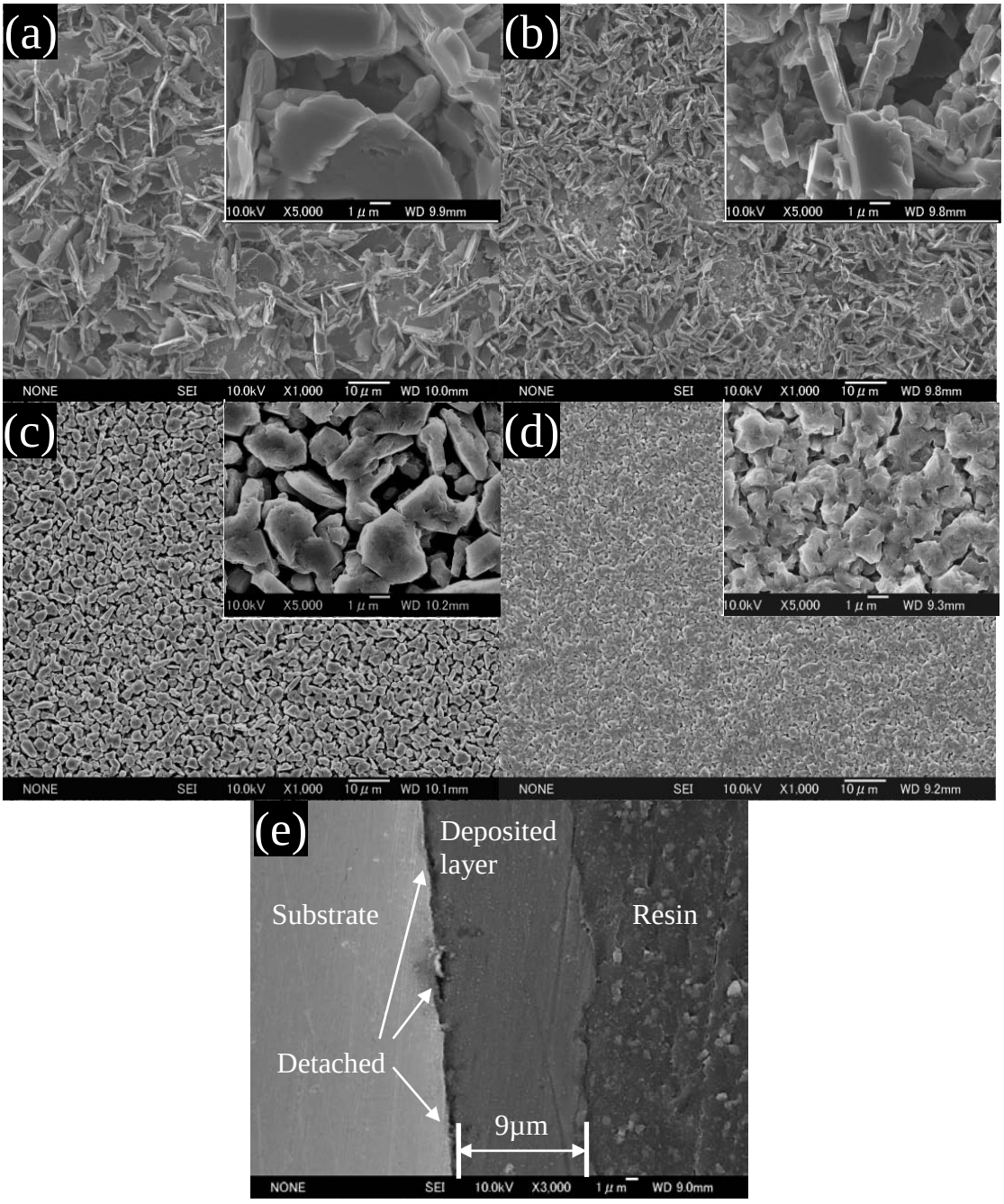

Fig. 6 SEM images of the Al surface electrodeposited from the [EMIm]Cl/$AlCl_3$ (0.5 mol%) bath using galvanostatic polarization at (a) -3.0 mA cm^{-2}, (b) -4.5 mA cm^{-2}, (c) -6.0 mA cm^{-2}, and (d) -8.0 mA cm^{-2}. (e) Cross-sectional SEM image of (d).

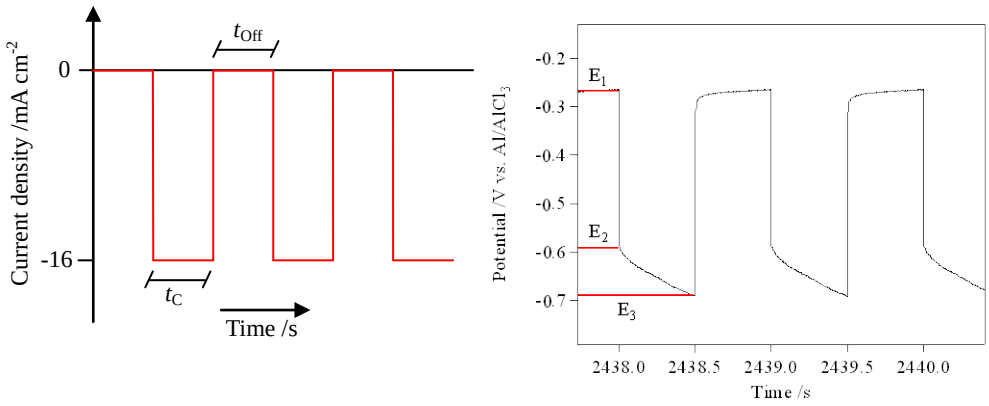

Fig. 7 Current pulse waveform for Al electrodeposition and potential response during MCP polarization.

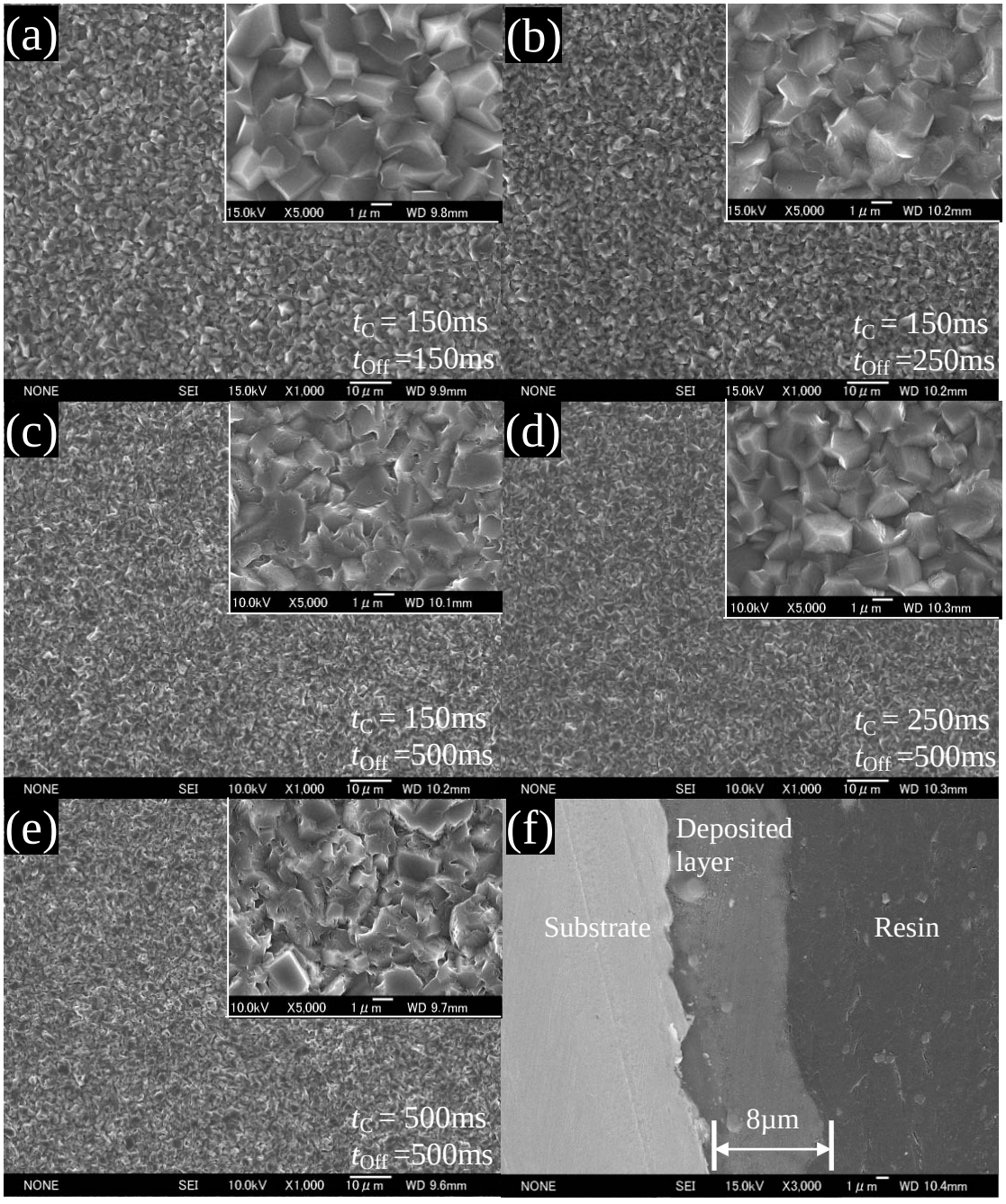

Fig. 8 SEM images of the Al surface electrodeposited from the [EMIm]Cl/$AlCl_3$ (0.5 mol%) bath using the MCP method at I_C = -16.0 mA cm^{-2}. (a) r_C = 0.5, f = 3.3 Hz; (b) r_C = 0.375, f = 2.5 Hz; (c) r_C = 0.23, f = 1.54 Hz; (d) r_C = 0.33, f = 1.33 Hz; (e) r_C = 0.5, f = 1 Hz. (f) Cross-sectional SEM image of (c).

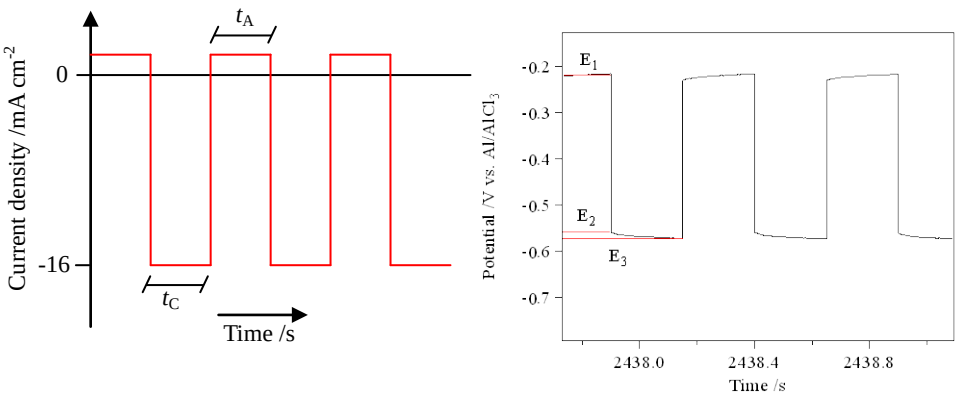

Fig. 9 Current pulse waveform for Al electrodeposition and potential response during BCP polarization.

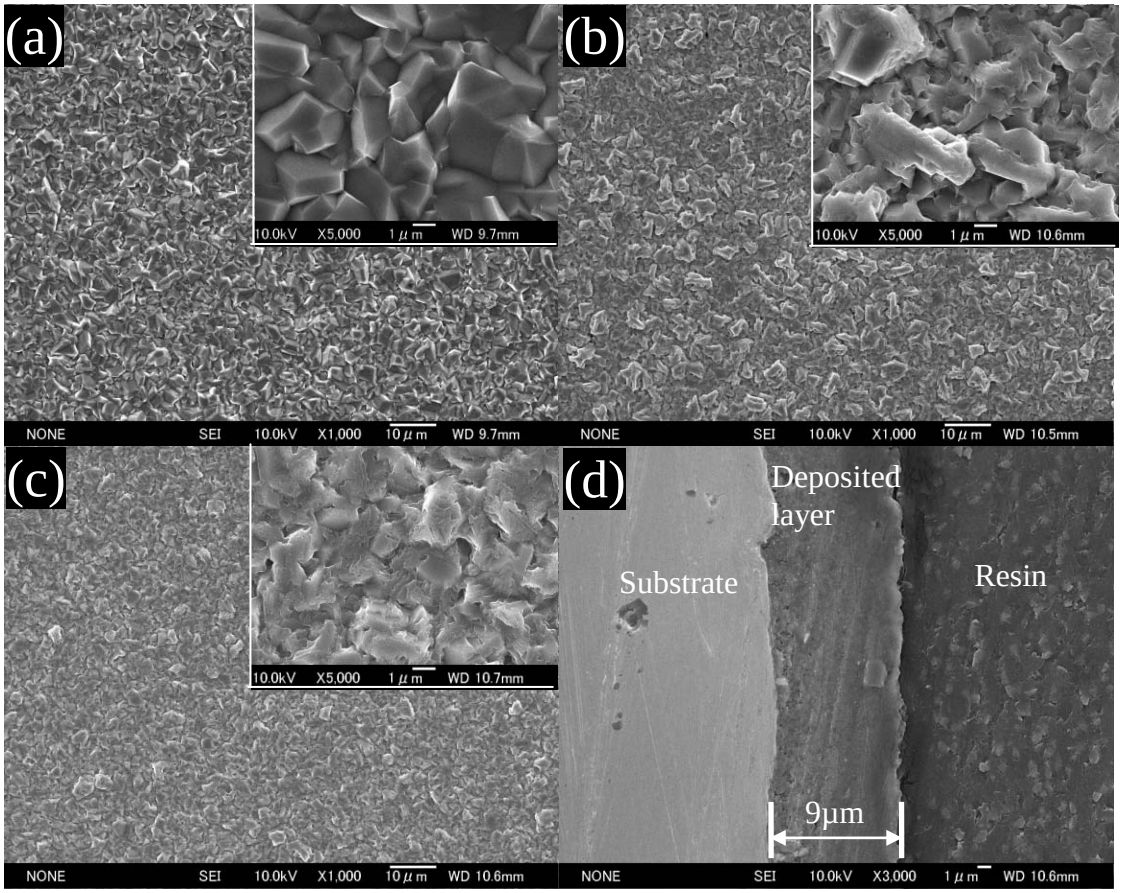

Fig. 10 SEM images of the Al surface electrodeposited from the [EMIm]Cl/$AlCl_3$ (0.5 mol%) bath using the BCP method with duty ratio r_C = 0.5, f = 2 Hz, cathodic current density I_C = -16 mA cm^{-2}, and anodic current density I_A = (a) 0.3, (b) 0.5, and (c) 1.0 mA cm^{-2}. (d) Cross-sectional SEM image of (c).

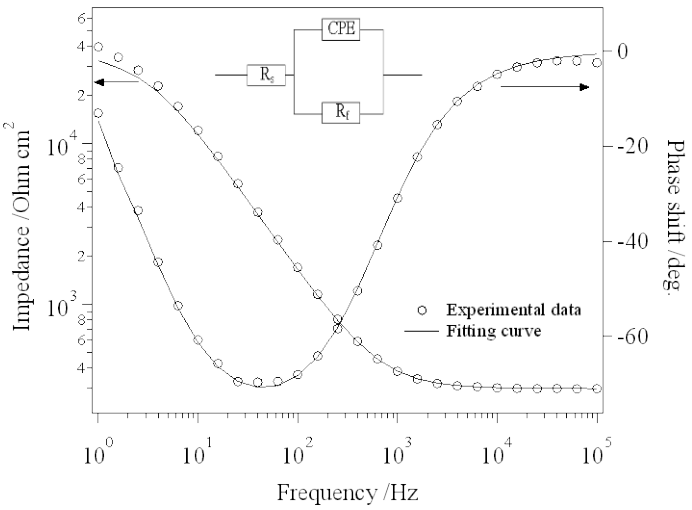

Fig. 11 Bode diagram of Al deposits obtained from the [EMIm]Cl/$AlCl_3$ (0.5 mol%) bath using the MCP method with the conditions of r_C = 0.5, f = 3.3 Hz.

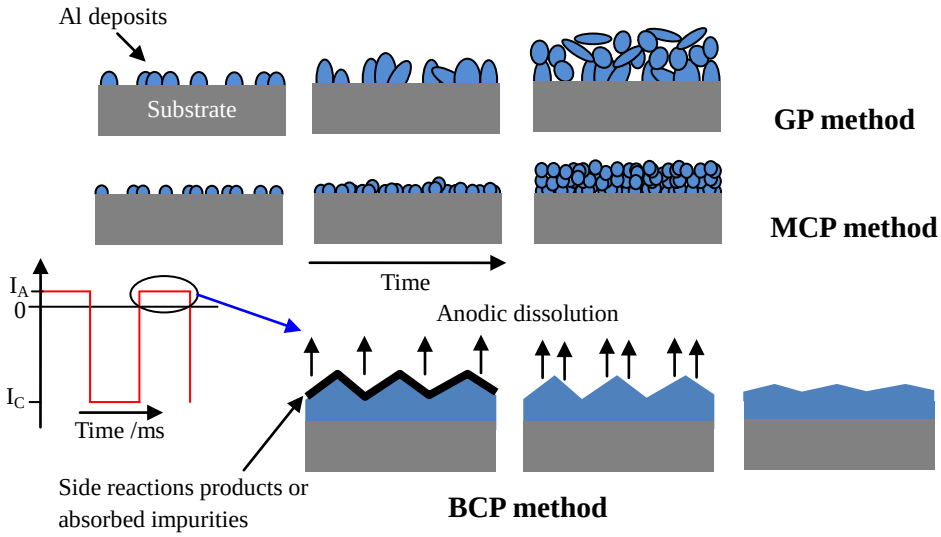

Fig. 12 (Color online) Schematic representation of growth of Al electrodeposited from the [EMIm]Cl/$AlCl_3$ (0.5 mol%) bath by using the GP, MCP and BCP methods.